Control Authority of a Projectile Equipped With an Internal Unbalanced Part

Geoffrey Frost
Graduate Research Assistant
ORISE Fellow

Mark Costello
Associate Professor
Mem. ASME

Department of Mechanical Engineering,
Oregon State University,
Corvallis, OR 97331

A key technical challenge for smart weapon developers is the design of appropriate control mechanisms that provide sufficient control authority to enable correction of typical trajectory errors while not excessively burdening the overall weapon design. The work reported here considers a rotating mass unbalance control mechanism, created by radial orientation of an internal part. To investigate the potential of this control mechanism, a seven degree-of-freedom flight dynamic model of a projectile, equipped with an internal part is defined. Using this dynamic model it is shown that by holding the internal part fixed with respect to a nonrolling reference frame, predictable trajectory changes are generated including predictable impact point changes. As expected, when unbalance-offset distance, or mass is increased, control authority increases proportionally. This control mechanism creates impact point changes that are the same order of magnitude as dispersion caused by errors induced at launch and in flight. Control authority is significantly altered with changing projectile characteristics, such as, the mass center location, pitch inertia, yaw inertia, aerodynamic drag, and aerodynamic normal force. [DOI: 10.1115/1.2363205]

Introduction

As the range of uncontrolled weapons is increased, a side effect is a concomitant increase in impact point dispersion. To statistically neutralize a target, the number of rounds to be fired by a conventional weapons system is directly proportional to the impact point dispersion of the system. Thus, the price to pay for increased projectile range is firing more rounds at the target [1,2]. To circumvent this basic limitation of conventional weapon systems, designers are considering employing active control technology to simultaneously enable both increased range and decreased dispersion for future systems. A key component of a smart projectile is the control mechanism. The control mechanism must be capable of altering the trajectory of the projectile in such a way that impact point errors induced at launch and in flight can be corrected. At the same time, the control mechanism must be rugged to withstand high acceleration loads at launch, small so that payload space is not compromised, and inexpensive for cost considerations.

Current projectile control mechanisms include configurations capable of manipulating aerodynamic loads, generating jet thrust, and altering inertial loads on the body. Examples of aerodynamic control mechanisms include rotation of aerodynamic lifting surface appendages, deflection of the nose, and deflection of ram air to side ports. Examples of jet thrust control mechanisms include gas jet thrusters, and explosive thrusters. Examples of inertial control mechanisms include internal translation of a control mass and internal rotation of an unbalanced part.

Many conventional uncontrolled projectile configurations contain internal parts that move slightly in flight. For example, submunitions deployed from indirect fire projectiles are keyed into place inside the round, however, small relative motion occurs. Also, fuse mechanisms used on some indirect fire ammunition employ a rotor that is permitted to move slightly with respect to the main projectile body. Although seemingly insignificant from a dynamic modeling perspective, small mass unbalances in these configurations can induce instability of the round as a whole typified in flight by a large loss in range and large spin decay. For this reason, several researchers have investigated dynamic stability of projectiles with moving internal components [3]. Soper [4] evaluated the stability of a spinning projectile that contains a cylindrical mass fitted loosely into a cylindrical cavity. Using a similar geometric configuration, Murphy [5] developed a quasilinear solution for a projectile with an internal moving part. Later, D'Amico [6] performed a detailed series of experiments where a projectile with a loose internal part was driven by the rotor of a freely gimbaled gyroscope. Hodapp [7] expanded the work of Soper [4] and Murphy [5] by considering a projectile configuration with a partially restrained internal member with a mass center offset.

Some new projectile configurations are designed with sizable moving parts that are fundamental to the operation of the projectile. For example, the gimbal nose projectile configuration mounts the nose section on a gimbal joint so that the nose is capable of rotating freely with respect to the main body of the projectile. Several investigations have evaluated the potential of the gimbal nose concept to be used as a control mechanism and a means to reduce dispersion [8–10]. Another example of a multiple component configuration is the dual-spin projectile which consists of forward and aft sections connected through a bearing allowing different spin rates for each section. The utility of the configuration has emerged for guided spin stabilized rounds where the control mechanism is isolated from the rapidly rotating main body [11–13].

The work reported here evaluates control authority of fin-stabilized and spin-stabilized projectiles equipped with an internal part that can be controlled to an arbitrary roll orientation. At launch, the part is assumed to be symmetric, and located on the projectile axis of symmetry in order to avoid trajectory changes due to lateral throw-off. Before the control mechanism is deployed, it is rotated to the desired roll orientation. The unbalance is subsequently deployed yielding an unbalanced configuration. By holding the part in different roll orientations with respect to a nonrolling reference frame, predictable trajectory changes occur, suggesting a potential control mechanism. The effects of varying inertia and aerodynamic properties of a nominal rigid projectile are studied. The paper begins with the description of a seven-degree of freedom flight dynamic model used for trajectory predictions along with the description of a flight control system to track commanded roll orientation of the part. The model is subsequently employed to predict control authority of exemplary fin-stabilized and spin-stabilized projectiles and of the same projectiles modified such that their inertia and aerodynamic properties are more responsive to control. Control authority versus the radial offset, activation time, mass of unbalance, and system velocity, is documented.

Internal Part Projectile Dynamic Model

A modified projectile containing an internal part and a mechanism capable of actively controlling the angular position of that part about its axle is considered as shown in Fig. 1. The modified

Contributed by the Dynamic Systems, Measurement, and Control Division of ASME for publication in the JOURNAL OF DYNAMIC SYSTEMS, MEASUREMENT, AND CONTROL. Manuscript received September 11, 2004; final manuscript received January 8, 2006. Assoc. Editor: Ranjan Mukherjee.

Copyright © 2006 by ASME

Downloaded From: http://dynamicsystems.asmedigitalcollection.asme.org/ on 07/23/2014 Terms of Use: http://asme.org/terms

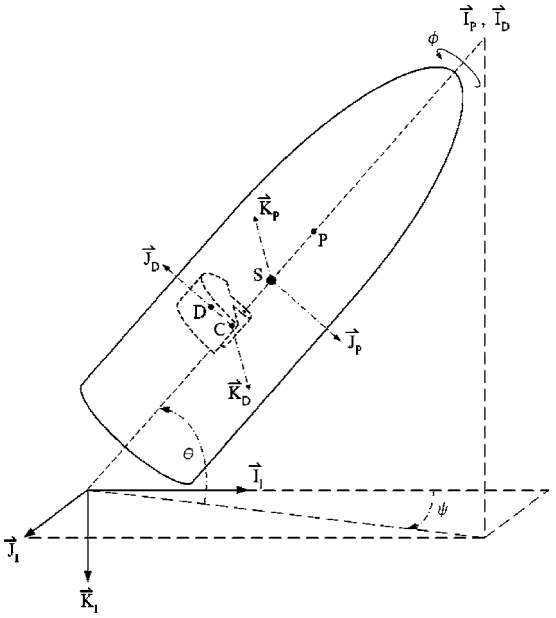

Fig. 1 Example system configuration

projectile is identified simply as the projectile and its center of mass is identified by the point "*P*." The projectile (*P*) and the internal part (*D*) are both rigid bodies, connected at an arbitrary point (*C*). The motion of the part is constrained to rotate about its axle. Figure 1 shows the relative locations of the centers of mass for the projectile, part, and initially symmetrical system (*S*). The mathematical model describing the motion of the system allows for seven rigid-body degrees of freedom. Three translational and three rotational degrees of freedom are used to describe the motion of the main body and one rotational degree of freedom is used to describe the angular motion of the part with respect to the modified projectile body. In order to develop the dynamic equations of motion for these seven degrees of freedom, three separate reference frames are used as shown in Fig. 1. The ground surface is used as an inertial reference frame with $\mathbf{K}_I$ positive down. A body frame is fixed on the projectile at the system reference point with $\mathbf{I}_P$ positive out the nose of the projectile. Another body frame is fixed on the internal moving part at the center of the part and axle joint, such that $\mathbf{I}_D$ lies along the axle of the part. The part is considered attached to the axle, and the axle affixed to an actuator mechanism that is rigidly attached to the projectile. The part body frame is initially coincident with the projectile body frame and is oriented with respect to the projectile body through the rotation angle ϕ_D.

Applying the projectile body frame to inertial frame transformation to the mass center velocity vector yields the translational kinematic differential equations,

$$\begin{Bmatrix} \dot{x} \\ \dot{y} \\ \dot{z} \end{Bmatrix} = T_P \begin{Bmatrix} u \\ v \\ w \end{Bmatrix} \tag{1}$$

$$T_P = \begin{bmatrix} c_\theta c_\psi & s_\phi s_\theta c_\psi - c_\phi s_\psi & c_\phi s_\theta c_\psi + s_\phi s_\psi \\ c_\theta s_\psi & s_\phi s_\theta s_\psi + c_\phi c_\psi & c_\phi s_\theta s_\psi - s_\phi c_\psi \\ -s_\theta & s_\phi c_\theta & c_\phi c_\theta \end{bmatrix} \tag{2}$$

Equating the angular velocity components, using Euler angle time derivatives and body frame angular velocity components yields the rotation kinematic differential equations,

$$\begin{Bmatrix} \dot{\phi} \\ \dot{\theta} \\ \dot{\psi} \\ \dot{\phi}_D \end{Bmatrix} = \begin{bmatrix} 1 & s_\phi t_\theta & c_\phi t_\theta & 0 \\ 0 & c_\phi & -s_\phi & 0 \\ 0 & s_\phi / c_\theta & c_\phi / c_\theta & 0 \\ 0 & 0 & 0 & 1 \end{bmatrix} \begin{Bmatrix} p \\ q \\ r \\ \omega \end{Bmatrix} \tag{3}$$

The kinematic differential equations define seven of the 14 dynamic equations needed to describe the trajectory of the states. The remaining seven differential equations are derived by separating the two-body system at the part axle connection point and considering the reaction forces and moments associated with each individual body. A constraint force $\mathbf{F}_R$ and a constraint moment $\mathbf{M}_R$ applied at the connection point *C* couple the part and projectile bodies. Axial moments, $\mathbf{T}$ and $\mathbf{M}_F$, due to torque generated by the controlling mechanism and bearing friction are applied to the bodies. The projectile body is also acted on by aerodynamic forces, $\mathbf{F}_A$ and aerodynamic moments, $\mathbf{M}_A$. The translational dynamic equations of motion for each body are given in Eqs. (4) and (5),

$$m_D \mathbf{a}_{D/I} = \mathbf{F}_R + \mathbf{W}_D \tag{4}$$

$$m_P \mathbf{a}_{P/I} = -\mathbf{F}_R + \mathbf{W}_P + \mathbf{F}_A \tag{5}$$

Summing Eqs. (4) and (5) eliminates the reaction force and yields the translational dynamic equation of motion describing the acceleration of the center of mass of the two-body system. When expressed in component form in the projectile body frame it yields three translational kinetic differential equations.

$$m_P \mathbf{a}_{P/I} + m_D \mathbf{a}_{D/I} = \mathbf{W}_D + \mathbf{W}_P + \mathbf{F}_A \tag{6}$$

The acceleration of the mass center of the projectile $\mathbf{a}_{P/I}$ is expressed in terms of the acceleration of the stationary system reference point, *S*, by applying the formula for two points fixed on a rigid body from the stationary system reference point to the projectile mass center,

$$\mathbf{a}_{P/I} = \mathbf{a}_{S/I} + \boldsymbol{\alpha}_{P/I} \times \mathbf{r}_{S\to P} + \boldsymbol{\omega}_{P/I} \times (\boldsymbol{\omega}_{P/I} \times \mathbf{r}_{S\to P}) \tag{7}$$

where

$$\mathbf{a}_{S/I} = \frac{{}^P d\mathbf{V}_{S/I}}{dt} + \boldsymbol{\omega}_{P/I} \times \mathbf{V}_{S/I} \tag{8}$$

The acceleration of the mass center of the part $\mathbf{a}_{D/I}$ is expressed in terms of the acceleration of the stationary system reference point, *S*, by applying the formula for two points fixed on a rigid body from the stationary system reference point to the connection joint *C*, and again from the connection joint to the part mass center *D*,

$$\mathbf{a}_{D/I} = \mathbf{a}_{S/I} + \boldsymbol{\alpha}_{P/I} \times \mathbf{r}_{S\to C} + \boldsymbol{\omega}_{P/I} \times (\boldsymbol{\omega}_{P/I} \times \mathbf{r}_{S\to C}) + \boldsymbol{\alpha}_{D/I} \times \mathbf{r}_{C\to D} + \boldsymbol{\omega}_{D/I} \times (\boldsymbol{\omega}_{D/I} \times \mathbf{r}_{C\to D}) \tag{9}$$

The angular accelerations with respect to the inertial frame of the projectile body, $\boldsymbol{\alpha}_{P/I}$, and the part body, $\boldsymbol{\alpha}_{D/I}$, is found by taking the derivatives of the respective angular velocities,

$$\boldsymbol{\alpha}_{P/I} = \frac{{}^P d\boldsymbol{\omega}_{P/I}}{dt} + \boldsymbol{\omega}_{P/I} \times \boldsymbol{\omega}_{P/I} = \frac{{}^P d\boldsymbol{\omega}_{P/I}}{dt} \tag{10}$$

$$\boldsymbol{\alpha}_{D/I} = \frac{{}^P d\boldsymbol{\omega}_{P/I}}{dt} + \frac{{}^P d\boldsymbol{\omega}_{D/P}}{dt} + \boldsymbol{\omega}_{P/I} \times \boldsymbol{\omega}_{D/P} \tag{11}$$

Summing the moments acting on the part about the connection point *C* yields the rotational equation of motion for the part body. The rotational dynamic equation of motion for the projectile body is found by summing the moments about the projectile mass center,

$$\frac{{}^I d\mathbf{H}_{D/I}}{dt} + \mathbf{r}_{C\to D} \times \mathbf{a}_{D/I} = \mathbf{T} + \mathbf{M}_R + \mathbf{r}_{C\to D} \times \mathbf{W}_D - \mathbf{M}_F \tag{12}$$

Downloaded From: http://dynamicsystems.asmedigitalcollection.asme.org/ on 07/23/2014 Terms of Use: http://asme.org/terms

$$\frac{{}^{I}d\mathbf{H}_{P/I}}{dt} = \mathbf{M}_A - \mathbf{T} - \mathbf{M}_R - \mathbf{r}_{P\to C} \times \mathbf{F}_R + \mathbf{M}_F \tag{13}$$

Summing Eqs. (12) and (13) eliminates the reaction moments and forms the rotational dynamic equation of motion for the two-body system. This equation yields three rotational kinetic differential equations. In component form it is expressed in the projectile body frame,

$$\frac{{}^{I}d\mathbf{H}_{P/I}}{dt} + \frac{{}^{I}d\mathbf{H}_{D/I}}{dt} = \mathbf{M}_A - \mathbf{r}_{C\to D} \times \mathbf{a}_{D/I} - \mathbf{r}_{P\to C} \times \mathbf{F}_R + \mathbf{r}_{C\to D} \times \mathbf{W}_D \tag{14}$$

The constraint force is obtained by subtracting Eq. (5) from Eq. (4),

$$\mathbf{F}_R = \left(\mathbf{a}_{D/I} - \mathbf{a}_{P/I} + \frac{\mathbf{F}_A}{m_P}\right)\left(\frac{m_D m_P}{m_D + m_P}\right) \tag{15}$$

The aerodynamic loads $\mathbf{F}_A$ and moments $\mathbf{M}_A$ exerted on the projectile body in the above equations are found using standard aerodynamic theory for projectiles [14].

The derivatives of angular momentum of the bodies are given in Eqs. (16) and (17)

$$\frac{{}^{I}d\mathbf{H}_{D/I}}{dt} = \frac{{}^{P}d\mathbf{H}_{D/I}}{dt} + \boldsymbol{\omega}_{P/I} \times \mathbf{H}_{D/I} \tag{16}$$

$$\frac{{}^{I}d\mathbf{H}_{P/I}}{dt} = \frac{{}^{P}d\mathbf{H}_{P/I}}{dt} + \boldsymbol{\omega}_{P/I} \times \mathbf{H}_{P/I} \tag{17}$$

The final kinetic differential equation is found by summing the axial moments acting on the part. This is accomplished by dotting each term of the rotational dynamic equation of motion of the part body with the unit vector $\mathbf{I}_D$ of the disk body frame. An axle joint cannot support an axial constraint moment, and therefore the reaction moment $\mathbf{M}_R$ does not appear in the equation,

$$\mathbf{I}_D \cdot \frac{{}^{I}d\mathbf{H}_{D/I}}{dt} + \mathbf{I}_D \cdot (\mathbf{r}_{C\to D} \times \mathbf{a}_{D/I}) = \mathbf{I}_D \cdot \mathbf{T} + \mathbf{I}_D \cdot (\mathbf{r}_{C\to D} \times \mathbf{W}_D) - \mathbf{M}_F \tag{18}$$

The independent state variables, x, y, z, ϕ, θ, ψ, and ϕ_D, are defined by the kinematic differential equations. The variables u, v, w, p, q, r, and ω are chosen for the remaining seven states variables where (u,v,w) are the projectile body frame components of the composite body mass center with respect to an inertial frame, (p,q,r) are the projectile body frame components of the angular velocity of the projectile relative to an inertial frame, and ω is the spin rate of the rotating internal part relative to the projectile body. The seven kinetic differential equations are found by expressing the dynamic equations of motion given by Eqs. (6), (14), and (18) in component form.

Projectile and Two-Body System Mass and Inertia Properties

To properly compare the effects on the trajectory of a projectile containing an asymmetrical internal part to that of a rigid projectile, special consideration is given to the formulation of the system's mass and inertial properties. The total mass and inertia properties of the two-component system are held constant at values equal to that of a baseline rigid projectile. A disk-shaped mass, located on the axis of symmetry of the baseline rigid projectile, is removed. The removed mass is equal to that of the internal part and the resulting mass and inertia properties of the baseline rigid projectile are appropriately modified. The internal part is then added to the projectile such that if the internal part were held fixed with respect to the projectile body the combined masses produce mass and inertia properties for the two-body system that are identical to the baseline rigid projectile. The reference point, "*S*," is taken as the center of mass of the baseline rigid projectile and is fixed at an equivalent location on the modified projectile. The original baseline projectile is called the nominal rigid projectile in the results section.

Unbalanced Part Roll Control

For a gun-launched weapon, acceleration at the muzzle exit is sufficiently large to prevent proper operation of the on-board CPU until slightly after launch, as well as prevent relative motion between the projectile and internal part. If the internal part is laterally offset from the projectile axis of symmetry at the time of firing the two-body system is equivalent to a statically unbalanced projectile. A statically unbalanced projectile while traveling down a rifled gun barrel is mechanically constrained to rotate about its geometric center of form. At the muzzle of the gun, the mechanical constraint provided by the barrel is suddenly removed, and the initial conditions of the free-flight trajectory are dependent on the spin rate, the lateral offset of the center of mass, and the roll orientation angle of the center of mass. The effect of a lateral center-of-mass offset, or static unbalance is to change the initial direction of the trajectory of a spin-stabilized projectile at the gun muzzle [15]. Exterior ballisticians commonly refer to this effect as lateral throw-off. Internal part offset from the projectile axis of symmetry at launch results in unpredictable changes in the trajectory because roll angle of the mass center is not practically controllable at the muzzle. To avoid lateral throw-off effects, the internal part's center of mass is located on the projectile axis of symmetry, and the part is symmetric and not spinning relative to the projectile. After the system exits the muzzle the control-processing unit is powered on and a small amount of time is allowed to elapse in order for the system to warm up. The symmetric part is controlled to the desired roll orientation relative to a nonrolling reference frame, reformed as an asymmetrical part, and offset from the axis of symmetry inducing a stationary mass unbalance in the two-body system.

A proportional-plus-derivative controller is used to control the unbalance part relative to the nonrolling reference frame. Equation (19) provides an expression for the roll angle error that circumvents problems with angle wrapping,

$$\phi_E = \tan^{-1}\left(\frac{s_{\phi_J} c_{\phi_C} - c_{\phi_J} s_{\phi_C}}{c_{\phi_J} c_{\phi_C} + s_{\phi_J} s_{\phi_C}}\right) \tag{19}$$

Control of the error is maintained by applying an axial torque $\mathbf{T}$.

The main mechanism for steering the system is a moment produced by axial drag about the composite body center of mass that is created by positioning the part in a fixed orientation relative to the nonrolling reference frame attached to the projectile body. This moment causes a fin-stabilized system to swerve in the same direction of the resulting yawing motion. However, for a spin-stabilized system, the swerve is approximately 180 deg out of phase with the initial direction of the yaw due to the gyroscopic effects inherent in a spinning projectile. Thus, positioning the part to the right of the projectile centerline will cause a spin-stabilized system to swerve to the right and up.

Results

To generate trajectories, and resulting impact data, the fourteen differential equations described above are numerically integrated using a fourth order Runge-Kutta algorithm. In order to validate the dynamic model, trajectory results were generated for the special case of a symmetric disk mounted on the axis of symmetry of the projectile. Bearing friction was set sufficiently large so that relative motion between the disk and projectile was negligible, hence mimicking a rigid projectile. These trajectory results compared favorably with a well-known rigid 6 DOF model driven by the same configuration data.

Downloaded From: http://dynamicsystems.asmedigitalcollection.asme.org/ on 07/23/2014 Terms of Use: http://asme.org/terms

Table 1 System characteristics and flight conditions

Fin-Stabilized Systems		Spin-Stabilized Systems	
Common System Parameters		Common System Parameters	
Weight	120.020 N	Weight	422.00 N
Length	137.16 cm	Length	86.26 cm
Reference Diameter	6.99 cm	Reference Diameter	15.54 cm
Nominal System		Nominal System	
Center of Mass Location		Center of Mass Location	
Station Line Distance	76.20 cm	Station Line Distance	32.00 cm
Butt Line Distance	0.00 cm	Butt Line Distance	0.00 cm
Water Line Distance	0.00 cm	Water Line Distance	0.00 cm
Projectile Moments of Inertia		Projectile Moments of Inertia	
Roll Inertia	2.5E−2 kg m^2	Roll Inertia	0.48 kg m^2
Pitch Inertia	6.00 kg m^2	Pitch Inertia	6.21 kg m^2
Yaw Inertia	6.00 kg m^2	Yaw Inertia	6.21 kg m^2
Modified System		Modified System	
Center of Mass Location		Center of Mass Location	
Station Line Distance	46.22 cm	Station Line Distance	62.00 cm
Butt Line Distance	0.00 cm	Butt Line Distance	0.00 cm
Water Line Distance	0.00 cm	Water Line Distance	0.00 cm
Projectile Moments of Inertia		Projectile Moments of Inertia	
Roll Inertia	2.5E−2 kg m^2	Roll Inertia	0.61 kg m^2
Pitch Inertia	9.95 kg m^2	Pitch Inertia	5.35 kg m^2
Yaw Inertia	9.95 kg m^2	Yaw Inertia	5.35 kg m^2
Modified Drag System		Modified Drag System	
Aerodynamic Properties		Aerodynamic Properties	
Drag	Increased 30%	Drag	Increased 30%
Lift	N/A	Lift	Increased 30%
Internal Part		Internal Part	
Semicylinder	R=3.18 cm, L=10.16 cm	Semicylinder	R=6.35, L=6.35
Weight	17.79 N	Weight	44.91 N
Center of Mass Offset Dist.	1.35 cm	Center of Mass Offset Dist.	2.69 cm
Flight Conditions		Flight Conditions	
Roll Angle: 0 deg, Pitch Angle: 3 deg, Yaw Angle 0 deg		Roll Angle: 0 deg, Pitch Angle: 30 deg, Yaw Angle 0 deg	
Roll Rate: 50 rad/s, Pitch\Yaw Rate: 0.00 rad/s		Roll Rate: 1675 rad/s, Pitch\Yaw Rate: 0 rad/s	
Velocity: Forward 350.52 m/s, Side: 0.00 rad/s		Velocity: Forward 838.20 m/s, Side: 0.00 rad/s	
Part Control Initiation Time	0.5 s	Part Control Initiation Time	2.0 s
Mechanism Deployment Time	1.5 s	Mechanism Deployment Time	6.0 s
Part Command Angles	0 deg: 10 deg: 360 deg	Part Command Angles	0 deg: 10 deg: 360 deg

Mass, Inertia, and Aerodynamic Properties. Consideration is given to modifying the mass and inertia properties of the nominal rigid projectile such that it is fundamentally less stable than that of an exemplary fin-stabilized or spin-stabilized projectile. This modification is conducted to demonstrate the increased control authority achieved through destabilization of a nominal rigid projectile. Removing mass from the nominal rigid projectile and replacing it at a different location along the station line alters the mass and inertia properties. For a spin-stabilized projectile, this modification shifts the nominal rigid projectile center of mass forward and closer to the aerodynamic center of pressure and decreases the resistance to rotation about the $\mathbf{J}_P$ and $\mathbf{K}_P$ projectile body axes, while maintaining the nominal rigid projectile mass. For a fin-stabilized projectile, the nominal rigid projectile center of mass is shifted aft and closer to the aerodynamic center of pressure. The 7-DOF two-body system constructed with a nominal projectile is called the nominal two-body system and the 7-DOF two-body system constructed with a modified less stable projectile is called the modified two-body system. Consideration is also given to increasing the drag and lift on a modified and nominal system to further emphasize the increased control authority that is achieved by coupling this type of mechanism with nonstandard munition designs. These systems are called the modified drag system and the nominal drag system.

Fin-Stabilized Projectile. In order to determine the effects of using an internal part as a control mechanism for a fin-stabilized projectile the flight characteristics of a nominal, modified, and modified drag fin-stabilized system were simulated and compared to the flight characteristics of a standard rigid fin-stabilized projectile. The fin-stabilized system characteristics and initial flight conditions are shown in Table 1.

Rigid Fin-Stabilized Projectile Typical Trajectory. A rigid fin-stabilized rocket, given an initial 350.52 m/s forward velocity and a 50 rad/s roll rate, launched at an altitude of 500 m and a pitch angle of 3 deg, reaches a vertical plane target 3000 m away in approximately 11.5 s. The rocket's spin reverses direction in the initial 0.25 s of flight, and averages out at about −75 rad/s for the remainder of the flight. Its forward velocity decreases to approximately 225 m/s and it swerves less than 0.1 m laterally. A rigid fin-stabilized rocket impacts the target with an angle of attack that is less than 0.05 deg (see Figs. 2 and 3).

A typical part orientation angle time history for a commanded angle of 0.0 deg relative to the no-roll frame is shown in Fig. 4. When control is initiated at 0.5 s, torque is applied to the part causing it to rotate in a direction opposite to that of the projectile. The applied torque acts on the projectile in an equal and opposite direction causing it to spin down. Once control is implemented it takes approximately 0.2 s to reduce the roll rate of the part to less than 1 rad/s, and another 0.8 s to control the roll orientation of

Downloaded From: http://dynamicsystems.asmedigitalcollection.asme.org/ on 07/23/2014 Terms of Use: http://asme.org/terms

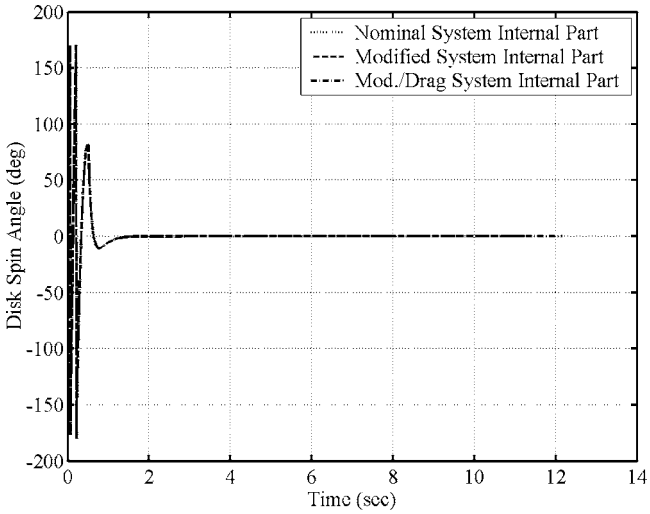

Fig. 2 Fin-stabilized system part roll angle time histories

the symmetrical part to the desired angle relative to the nonrolling reference frame as shown in Fig. 4. The maximum torque required to reduce the spin rate to less than 1 rad/s is approximately 0.30 N m as shown in Fig. 5. Once the roll rate of the part is reduced, and reformed asymmetrically at an offset from the projectile axis of symmetry, approximately half the maximum torque is necessary to control the disk at a specified angle.

Fin-Stabilized Projectile Control Authority. In order to evaluate control authority size and shape, vertical plane dispersion patterns are shown in Fig. 2 for different part command angles. Control authority is defined as the dispersion pattern created by the set of impact points. Control authority is shown for the nominal and modified two-body systems and for the nominal and modified two-body systems with 30% increased axial drag. For this study the orientation of the mass unbalance is controlled at angles from 0 to 360 deg in increments of 10 deg and impact points are plotted with respect to the impact points of similar uncontrolled systems. Predictable dispersion patterns are achieved for given mass unbalance orientation angles. Moreover, increased control authority is achieved by modifying the mass, inertia and aerodynamic properties of a rigid projectile such that it is fundamentally less stable than that of a typical fin stabilized projectile.

Fin-Stabilized Projectile Velocity Effects. In order to evaluate the effect that velocity has on a system containing an internal part, dispersion patterns were generated for a range of launch velocities of a modified fin-stabilized system fired at a pitch angle of 3 deg from an altitude of 3000 m at a target 3000 m down range. The effects of varying velocity are isolated from the time at which the internal mechanism is deployed by reforming the part asymmetrically at the same range (762 m) for each of the velocities. The radial mean of dispersion was calculated from the impact points generated by simulating the trajectories of the modified fin-stabilized system equipped with a semicylindrical part controlled at angles from 0 to 360 deg in increments of 10 deg. The radial mean of dispersion and average station line distance from the center of pressure to the system center of mass is plotted versus average velocity in Fig. 3. The increase in control authority at lower velocities is due to the fact that fin-stabilized systems usually become less stable at lower velocities, and therefore perturbation due to the axial drag induced moment results in a greater increase in yaw and consequently dispersion. The decrease in stability is a result of the Mach number dependent station line center of pressure approaching the system station line center of mass at lower velocity. This observable fact is shown in Fig. 3 where average station line distance from the center of pressure to the system station line center of mass is plotted versus velocity on the right-hand side of the graph. Consequences of increasing dispersion by lowering velocity are an increase in time to target and a loss in altitude.

Spin-Stabilized Projectile. In order to determine the effects of using an internal part as a control mechanism for a spin-stabilized projectile the flight characteristics of a nominal, modified, and modified drag fin-stabilized system were simulated and compared to the flight characteristics of a similar rigid spin-stabilized projectile. The spin-stabilized system characteristics and initial flight conditions are shown in Table 1.

Rigid Spin-Stabilized Projectile Typical Trajectory. A typical rigid spin-stabilized projectile, given an initial 838.20 m/s forward velocity and a 1674.00 rad/s roll rate, launched at a pitch angle of 30 deg, climbs to an altitude of approximately 4500 m impacting the ground approximately 60 s later at a distance of approximately 22 km downrange. Forward velocity decreases to approximately 300 m/s at the flight apex and then increases to approximately 320 m/s at the time of impact. Roll rate of the rigid projectile decreases over time to approximately 1100 rad/s at impact. The angle of attack approaches 0.7 deg at the apex and then diminishes to approximately 0.2 deg at impact.

Spin-Stabilized Projectile Control Authority. In order to evaluate the effect that controlling the orientation of the mass unbalance at different angles has on a spin-stabilized system, dispersion patterns shown in Fig. 6 are generated for the nominal, modified, and modified drag, two-body spin-stabilized systems. As in the fin-stabilized study the orientation of the mass unbalance is controlled at angles from 0 to 360 deg in increments of 10 deg. Ground impact points are plotted with respect to the impact points of a similar rigid projectile. The patterns are laterally shifted about the rigid projectile impact points because of the increased roll rates of the controlled systems. These axial torque induced roll rates produce Magnus forces that cause the controlled systems to swerve more laterally. Figure 6 is significant in the fact that it shows that predictable dispersion patterns are achieved for given mass unbalance orientation angles for a spin-stabilized system as well as for a fin-stabilized system. Increased control authority is also achieved with a spin-stabilized system by modifying the inertia and aerodynamic properties of the nominal rigid projectile such that it is fundamentally less stable than that of a typical spin stabilized projectile. Altering the aerodynamic properties changes the dynamics of the system such that the impact points for given angles are out of phase with the impact points generated from the same angles of a nonaerodynamically altered system.

Indirect Fire Weapon Pitch Angle Sensitivity. Figure 7 shows the dispersion patterns for a nominal spin-stabilized system fired at quadrant elevations of 15 deg, 30 deg, and 45 deg. Range control of an internal part control mechanism is limited in indirect fire weapons by the angle of fire. Changes in cross range are proportional to the quadrant elevation of the muzzle, however changes in range are sensitive to the pitch angle of the projectile. For a system fired at a quadrant elevation of 50 deg, any change in pitch angle affected by the internal mechanism produces very little change in range.

Part Mass and Offset Distance Effects. The effect of increasing part mass or increasing the distance the part center of mass is offset from the projectile axis of symmetry acts to increase control authority. However, the size and shape of the part is constrained by the size and shape of the projectile that it is contained within. A study was conducted in which material was removed in increasing radial amounts (as shown in Fig. 8) from a disk shaped part contained in a modified fin-stabilized system. Removing material from the disk results in a trade-off between increased mass center offset distance and decreased part mass. The radial mean of dispersion was calculated from the impact points generated by simu-

Downloaded From: http://dynamicsystems.asmedigitalcollection.asme.org/ on 07/23/2014 Terms of Use: http://asme.org/terms

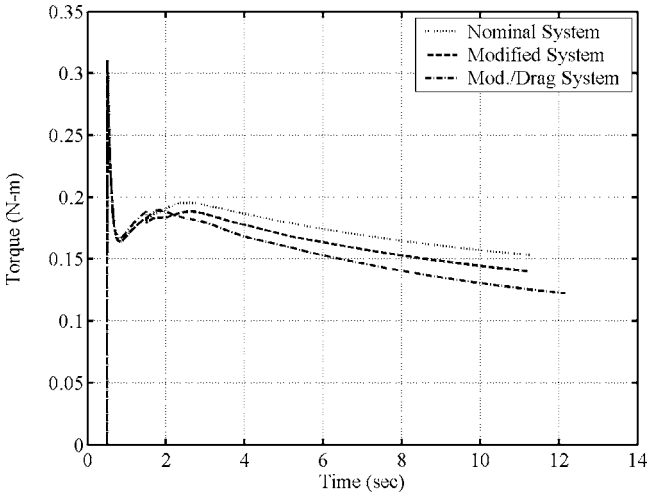

Fig. 3 Fin-stabilized system control torque

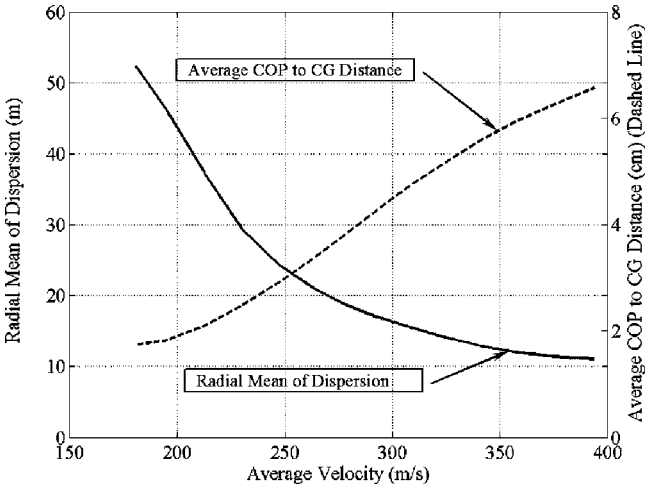

Fig. 5 Fin-stabilized dispersion and average station line distance versus average velocity

lating the trajectories of a modified fin-stabilized system equipped with the various parts controlled at angles from 0 to 360 deg in increments of 10 deg. By generating the dispersion patterns and calculating the radial mean it is shown in Fig. 9 that control authority is linearly proportional to the mass of the part times the radial offset of the part center of mass.

Mechanism Activation Time. In order to evaluate the effect that mechanism activation time has on control authority, dispersion patterns are shown for a modified spin-stabilized system fired at a quadrant elevation of 30 deg with nominal initial conditions. The allowable control torque was specified to be unlimited and the reformation time of the part was varied. The resulting radial mean of dispersion is plotted versus the part reformation time in Fig. 10. For an ideal system in which control torque is unlimited and the part is considered controlled at the desired orientation at firing, control authority achieved is greatly increased to a value of approximately 380 m. The amount of dispersion is greatly reduced as the time of part reformation is increased.

Conclusions

A seven-degree of freedom flight dynamic model is documented and subsequently used for trajectory predictions of fin-stabilized and spin-stabilized projectiles equipped with internal unbalanced rotating parts. It is shown that holding the unbalanced part in a fixed roll orientation with respect to the no-roll reference frame causes predictable trajectory changes with respect to an uncontrolled system including predictable impact point changes. The main mechanism for steering the projectile is a moment produced by axial drag about the composite body center of mass that is created by positioning the part in a fixed roll orientation. Control authority for both types of systems is shown to increase proportionally as the multiplicative value of unbalance-offset distance times part mass is increased. The amount of control authority

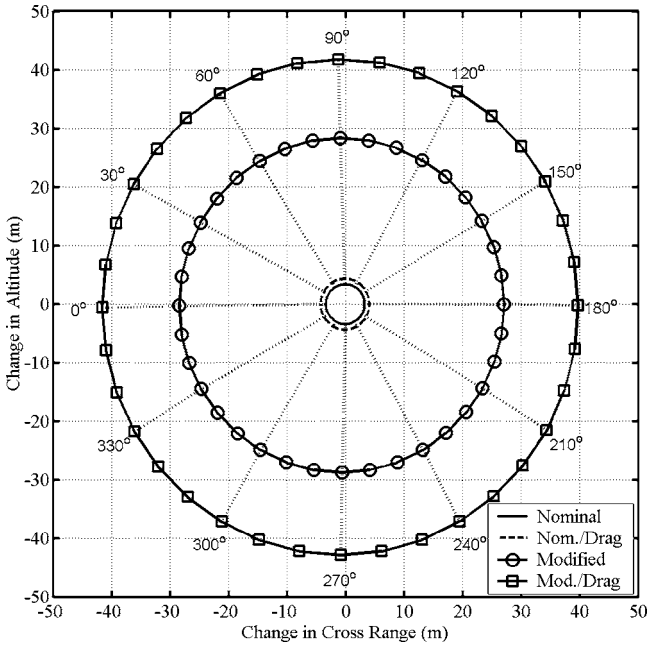

Fig. 4 Control authority of fin stabilized projectile (launch angle=3 deg)

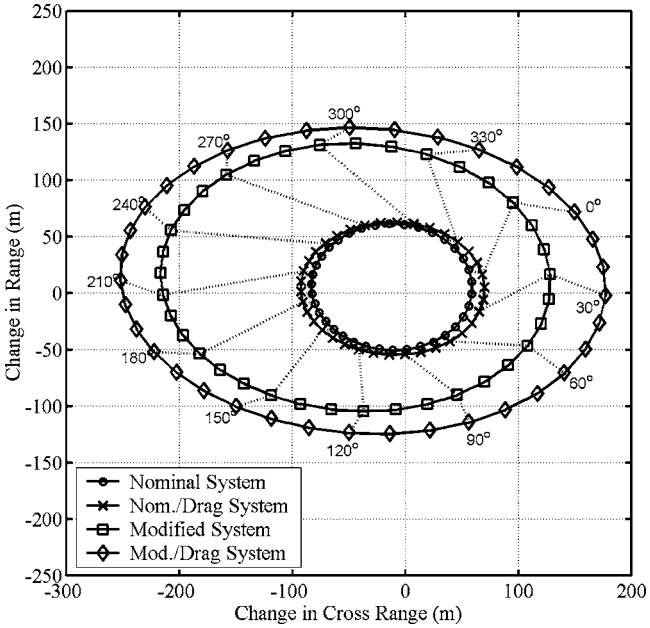

Fig. 6 Control authority of spin stabilized projectile (launch angle=30 deg)

Downloaded From: http://dynamicsystems.asmedigitalcollection.asme.org/ on 07/23/2014 Terms of Use: http://asme.org/terms

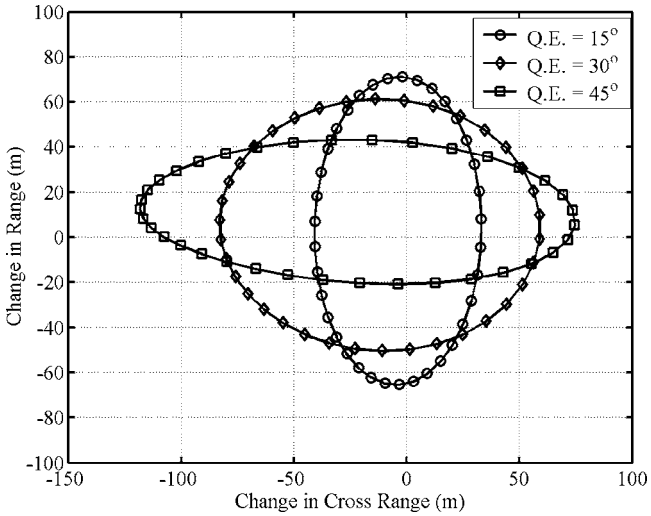

Fig. 7 Control authority for nominal spin stabilized system (launch angle=15 deg, 30 deg, and 45 deg)

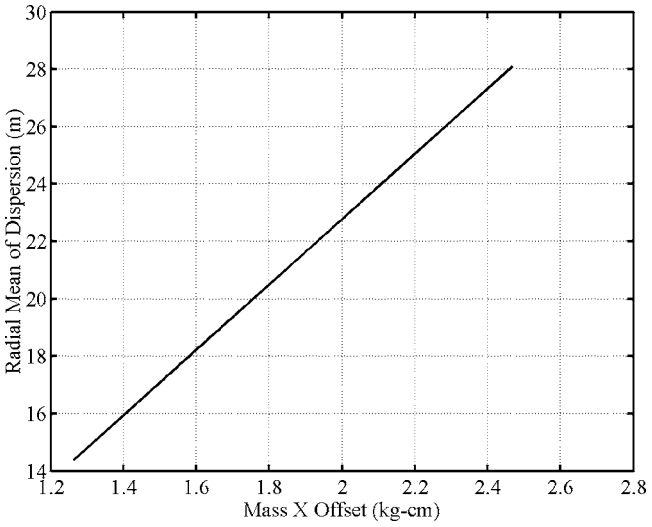

Fig. 9 Control authority versus part mass times part mass center offset

achieved is greatly increased the earlier in flight that control is initiated. Fin-stabilized system control authority is increased with lower average flight velocity, while spin-stabilized system control authority is increased with higher average flight velocity. The effect of decreasing or increasing the velocity in the appropriate system is to destabilize the projectile by moving the center of pressure closer to the center of mass such that it is more responsive to perturbations caused by axial drag induced moments. It should be noted that range control of an internal part control mechanism is limited in indirect fire weapons by the angle of fire. Changes in cross range are proportional to the quadrant elevation of the muzzle, however changes in range are sensitive to the pitch angle of the projectile. Significant increases in control authority are achieved when the control mechanism is combined with a basic projectile that is fundamentally less stable than current standard off-the-shelf weapons.

Nomenclature

$\mathbf{a}_{D/I}$ = acceleration of unbalanced part mass center with respect to an inertial frame
$\mathbf{a}_{P/I}$ = acceleration of projectile mass center with respect to an inertial frame
$\mathbf{a}_{S/I}$ = acceleration of stationary system reference point with respect to an inertial frame
$\boldsymbol{\alpha}_{D/I}$ = angular acceleration of unbalanced part with respect to an inertial frame
$\boldsymbol{\alpha}_{P/I}$ = angular acceleration of projectile with respect to an inertial frame
$\mathbf{F}_A$ = projectile aerodynamic forces
$\mathbf{F}_R$ = joint reaction force
$\mathbf{H}_{P/I}$ = angular momentum of the projectile with respect to an inertial frame
$\mathbf{H}_{D/I}$ = angular momentum of the unbalanced part with respect to an inertial frame
${}^C d\mathbf{h}/dt$ = general notation for time derivative of vector $\mathbf{h}$ observed from reference frame C
${}^I d/dt$ = indicates inertial frame time derivative
I_P = mass moment of inertia of the projectile about its mass center
I_D = mass moment of inertia of the unbalanced part about its mass center
$\mathbf{I}_C, \mathbf{J}_C, \mathbf{K}_C$ = control reference frame unit vectors
$\mathbf{I}_D, \mathbf{J}_D, \mathbf{K}_D$ = unbalanced part frame unit vectors
$\mathbf{I}_I, \mathbf{J}_I, \mathbf{K}_I$ = inertial frame unit vectors
$\mathbf{I}_N, \mathbf{J}_N, \mathbf{K}_N$ = no-roll frame unit vectors

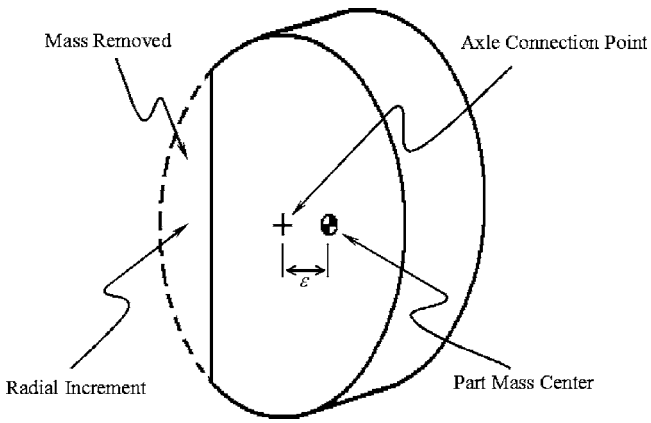

Fig. 8 Part mass removal configuration

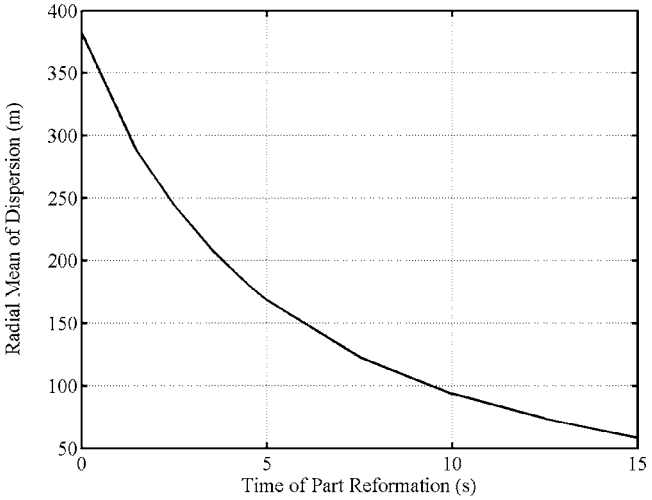

Fig. 10 Spin-stabilized dispersion versus time of part reformation

Downloaded From: http://dynamicsystems.asmedigitalcollection.asme.org/ on 07/23/2014 Terms of Use: http://asme.org/terms

$\mathbf{I}_P, \mathbf{J}_P, \mathbf{K}_P$ = projectile frame unit vectors
L_A, M_A, N_A = total aerodynamic moment components expressed in the projectile body frame
$\mathbf{M}_A$ = total aerodynamic moment expressed in the projectile body frame
$\mathbf{M}_F$ = bearing moment due to viscous friction expressed in the projectile body frame
$\mathbf{M}_R$ = bearing reaction moment expressed in the projectile body frame
m_D = unbalanced part body mass
m_P = projectile mass
${}^P d/dt$ = indicates projectile body frame time derivative
p, q, r = roll, pitch, and yaw components of the angular velocity vector of the projectile with respect to an inertial frame expressed in the projectile body frame
ϕ_C = commanded control angle
ϕ_E = control angle error
ϕ_J = part orientation angle
ϕ, θ, ψ = Euler roll, pitch, and yaw angles of projectile
$\mathbf{r}_{C \to D}$ = distance from internal part axle connection point to unbalanced part center of mass
$\mathbf{r}_{P \to A}$ = distance vector from projectile center of mass to center of pressure
$\mathbf{r}_{P \to C}$ = distance vector from projectile center of mass to unbalanced part axle connection point
$\mathbf{r}_{P \to D}$ = distance vector from projectile center of mass to unbalanced part center of mass
$\mathbf{r}_{P \to M}$ = distance vector from projectile center of mass to center of Magnus force
$\mathbf{r}_{S \to P}$ = distance vector from stationary system reference point to projectile center of mass
$\mathbf{r}_{S \to C}$ = distance vector from stationary system reference point to unbalanced part axle connection point
$\mathbf{T}$ = control torque vector
T_P = transformation matrix from the projectile body frame to the inertial frame
T_D = transformation matrix from the part body frame to the projectile body frame
u, v, w = translational velocity components of projectile center of mass resolved in the projectile body frame
$\mathbf{V}_{SI}$ = velocity of stationary system reference point with respect to the inertial frame
$\mathbf{W}_D$ = weight vector of part body
$\mathbf{W}_P$ = weight vector of projectile body
W_D = unbalanced part weight
W_P = projectile body weight
ω = unbalanced part spin rate relative to the projectile body angular velocity resolved in the unbalanced part frame
$\boldsymbol{\omega}_{D/I}$ = angular velocity of unbalanced part with respect to the inertial frame
$\boldsymbol{\omega}_{D/P}$ = angular velocity of unbalanced part with respect to the projectile body frame
$\boldsymbol{\omega}_{P/I}$ = angular velocity of projectile body with respect to the inertial frame
X_A, Y_A, Z_A = total aerodynamic force components expressed in the projectile body frame
x, y, z = position components of the projectile center of mass expressed in the inertial frame
x_{CD}, y_{CD}, z_{CD} = unbalanced part frame components of distance from part axle connection point to part center of mass expressed in the unbalanced part frame
x_{PC}, y_{PC}, z_{PC} = projectile body frame components of distance from projectile center of mass to part axle connection point expressed in the projectile body frame

References

[1] Richardson, D., 2003, "Summoning the Fire," Armada International, **27**(1), p. 10.
[2] Gander, T. J., 2003, "Artillery O Target—Trajectory Correctable Munitions," Armada International, **27**(2), p. 70.
[3] Murphy, C., 1981, "Symmetric Missile Dynamic Instabilities," J. Guid. Control, **4**(5), pp. 464–471.
[4] Soper, W., 1978, "Projectile Instability Produced by Internal Friction," AIAA J., **16**(1), pp. 8–11.
[5] Murphy, C., 1978, "Influence of Moving Internal Parts on Angular Motion of Spinning Projectiles," J. Guid. Control, **1**(2), pp. 117–122.
[6] D'Amico, W., 1987, "Comparison of Theory and Experiment for Moments Induced by Loose Internal Parts," J. Guid. Control, **10**(1), pp. 14–19.
[7] Hodapp, A., 1989, "Passive Means for Stabilizing Projectiles With Partially Restrained Internal Members," J. Guid. Control, **12**(2), pp. 135–139.
[8] Schmidt, E., and Donovan, W., 1998, "Technique to Reduce Yaw and Jump of Fin-Stabilized Projectiles," J. Spacecr. Rockets, **35**(1), pp. 110–111.
[9] Costello, M., and Agarwalla, R., 2000, "Improved Dispersion of a Fin Stabilized Projectile Using a Passive Moveable Nose," J. Guid. Control Dyn., **23**(5), pp. 900–903; **25**(2), p. 414(E).
[10] Smith, J., Smith, K., and Topliffe, R., 1978, "Feasibility Study for Application of Modular Guidance and Control Units to Existing ICM Projectiles," Final Technical Report, Contractor Report No. ARLCD-CR-79001, U.S. Army Armament Research and Development Command.
[11] Costello, M., and Peterson, A., 2000, "Linear Theory of a Dual Spin Projectile in Atmospheric Flight," J. Guid. Control Dyn., **23**(4), pp. 789–797.
[12] Burchett, B., Peterson, A., and Costello, M., 2002, "Prediction of Swerving Motion of a Dual-Spin Projectile With Lateral Pulse Jets in Atmospheric Flight," Math. Comput. Modell., **35**(7–8), pp. 821–834.
[13] Etkin, B., 1972, *Dynamics of Atmospheric Flight*, Wiley, New York, Chaps. 4 and 5.
[14] Arrow Tech Associates, Inc., 2002, PRODAS, Copyright © 1999–2002 Arrow Tech.
[15] McCoy, R. L., 1999, *Modern Exterior Ballistics*, Atglen, PA, Chaps. 2–12.

Downloaded From: http://dynamicsystems.asmedigitalcollection.asme.org/ on 07/23/2014 Terms of Use: http://asme.org/terms